Preparation, In-Vitro Evaluation, and Delivery of Colchicine *via* Polyacrylamide Hydrogel

Li, Xiaoxia
The College of Pharmacy, Anhui University of Chinese Medicine, Hefei 230012, Anhui, P.R. CHINA

Li, Yangyang
Department of General Surgery, the Fourth Affiliated Hospital of Anhui Medical University, No. 100 Huaihai Road, Hefei 230012, Anhui, P.R. CHINA

Wang, Min; Meng, Fanjun; Huang, Jinling; Yu, Rui; Wang, Yangying; Liu, Huanhuan*+
The College of Pharmacy, Anhui Province Key Laboratory of Pharmaceutical Preparation Technology and Application, Engineering Technology Research Center of Modernized Pharmaceutics, Anhui University of Chinese Medicine, Hefei 230012, Anhui, P.R. CHINA

ABSTRACT: *Hydrogels have excellent biocompatibility and are widely used in biomedical applications. However, it is still a challenge to build a hydrogel with outstanding mechanical properties and multiple functions. In this study, a polyacrylamide (PAM) hydrogel with a uniform network structure was achieved through an Ultra Violet (UV)-responsive organic crosslinking agent and a higher mechanical strength PAM-Ag^+ hydrogel was designed through the introduction of silver ion by metal coordination interaction. Various contents of N'N-bis(acryloyl)cysteamine (BACA) as cross-linker, acrylamide (AM) as a monomer, and Irgacure 2959 as initiator were investigated to have an optimal combination of high strength. Thus, the PAM-Ag^+ hydrogel exhibited excellent adhesive behavior that could be fixed to the human forearm and any part of the skin, such as the finger and elbow joint. In addition, the properties and biocompatibility evaluations of the tough hydrogel in medical wound dressing were investigated. Meanwhile, these results showed that PAM-Ag^+ hydrogels possess high stretchable (2600%) and mechanical robust (2.55 MPa) properties. Excitingly, the release of colchicine (Col) of more than 95% in 48 h demonstrated the hydrogel's high potential in medical dressing and drug release applications by the excellent moisture retention, permeability, water tightness, swelling ratio, and biocompatibility.*

KEYWORDS: *Hydrogels; High mechanical strength; Medical dressing; Drug release.*

INTRODUCTION

As a significant biological tissue, skin isolates the mechanical, chemical, and biological factors in the external environment and protects the body from being affected, prevents the loss of water, and regulates body temperature [1-4]. Thus, skin damage brings various inconveniences, and the resulting bacterial invasion and

***** *To whom correspondence should be addressed.*
+ *E-mail: huanhuanliu2016@ahtcm.edu.cn.*
1021-9986/2022/8/2595-2606 12/$/6.02

infection may lead to fluid loss and damage to function even threatening human life [5, 6]. Skin healing is a complex biological process including hemostasis and coagulation, inflammation, proliferation, and remodeling [1, 2]. The Medical dressing is generally applied to protect the wound from further infection through direct contact, provide good absorption of postoperative bleeding, and promote cell migration and epithelial regeneration [3]. In recent years, medical dressing has gradually expanded from traditional absorbents such as gauze to bioactive materials, including biomaterial-based dressings and artificial dressings [4]. The ideal medical dressing should promote healing with minimal inconvenience to the patient and new medical dressing design should be a great challenge to modern medicine [5, 7].

Similar to soft tissue, hydrogels with water content are hydrophilic macromolecule networks produced by chemical or physical crosslinking of soluble polymers, showing great potential as excellent candidates for medical dressing [8-14]. Since the poor mechanical and adhesive properties, Traditional hydrogels showed limited development in medical dressing. To overcome the above problems, nanocomposite hydrogels with uniform networks and outstanding mechanical properties have been designed and obtained for biomedical applications [15]. However, the weak interfacial interactions between the inorganic and organic matter limited the promotion of their mechanical performance [16]. Moreover, massive functional nanoparticles have been widely integrated into hydrogels. *Chen et al.* [17] reported a kind of mechanically strong, tough, and shape deformable poly (acrylamide-co-vinyl imidazole) hydrogels based on strong Cu^{2+} complexation with imidazole groups dramatically. *Yang et al.* [18] made the high-strength hydrogel by immersing the Na-alginate/PAAm hydrogel in metallic cation solutions in a two-step process. In addition, silver nanoparticles can promote wound healing based on their antimicrobial and anti-inflammatory activity [19-22]. Unfortunately, silver nanoparticles might be harmful to normal cells, which was confirmed by the finding of direct interaction between silver nanoparticles and living cells [23, 24]. In the last years, silver ions cooperated into functional hydrogels with antibacterial properties for biomedical materials [25-27]. Moreover, metal-ligand interaction was introduced to the hydrogels for advanced functionalities such as self-healing attributed to the dynamics [28-31]. The important factor of hydrogel design and preparation consists of finding the optimal formulation that yields the hydrogel with the best performance, such as excellent mechanical properties and biological activities. Furthermore, to the best of our knowledge, the evaluation of skin medical dressing derived from hydrogels based on *in vitro* assay and tensile properties was never reported for medical dressing. In addition to medical dressings, hydrogels also have promising applications in biomedicine [32], sensors [33], and environmental protection [34].

During this study, a tough and adhesive PAM hydrogel with a uniform network structure was prepared through an ultraviolet-responsive crosslinking agent. Combined with metal coordination, PAM-Ag^+ hydrogel with much enhanced mechanical performance was achieved through the introduction of silver ions via a simple deswelling/swelling process (Scheme 1). Different from traditional hydrogels, the network structure of the hydrogels showed evenly dispersed crosslinking points which could be attributed to the UV-responsive crosslinker, the excellent mechanical and adhesive properties of the hydrogels were ascribed to the dynamic metal coordination between sulfur and silver ions. Besides, a series of *in vitro* evaluations and delivery of colchicine with the target hydrogels were investigated, including moisture retention, permeability, water tightness, swelling property, skin irritation, and skin sensitization. Based on the above properties, the target hydrogel exhibited a great prospect in the application of medical dressings.

EXPERIMENTAL SECTION

Materials

Acrylamide (AM, Aladdin, ≥98%), N, N'-bis(acryloyl) cysteamine (BACA, Alfa Aesar, 98%), N, N'-methylene bisacrylamide (MBA, Alfa Aesar, 98%), 2-Hydroxy-4′-(2-hydroxyethoxy)-2-methylpropiophenone (Irgacure 2959, Sigma-Aldrich, 98%), $AgNO_3$ (Aladdin, 99%), all the water used in this study was Milli-Q purified water.

Preparation of PAM and PAM-Ag^+ Hydrogels

Pure PAM hydrogel was synthesized by the following procedure according to the relevant literature [35]. Firstly, desired amounts of monomer AM, crosslinker BACA, and photo-initiator Irgacure 2959 were completely dissolved in water orderly, with the assistance of ultra-sonication, and a transparent solution was produced finally. The detailed

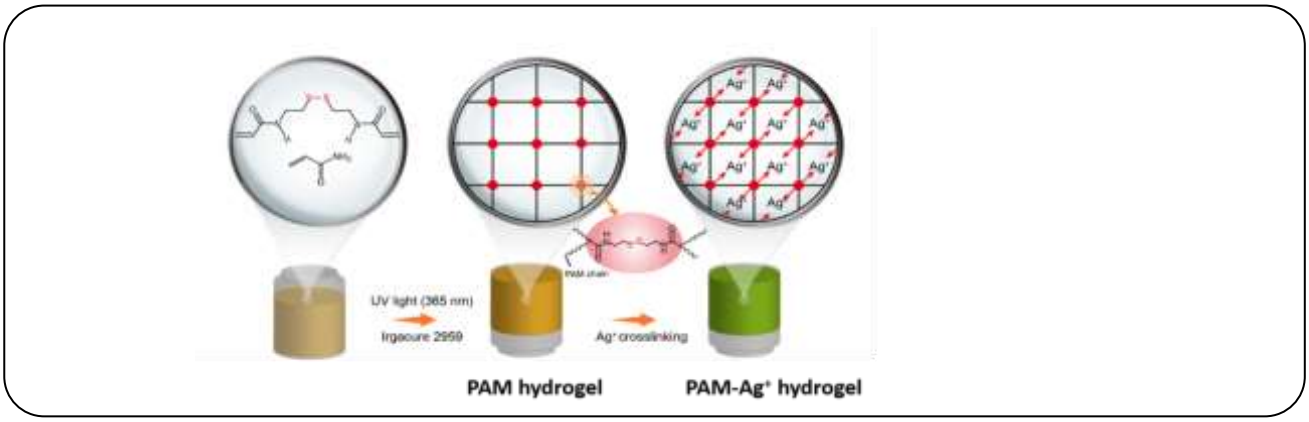

Scheme 1: Schematic illustration for the preparation of the PAM hydrogel by one-pot radical polymerization under UV irradiation and the PAM-Ag$^+$ hydrogel by a two-step process.

proportions were shown in table 1. Secondly, the solution was quickly transferred into a 25 mm diameter cylindrical mold and placed in high-energy UV irradiation (365 nm, 300 W) for 30 min to polymerize a pure PAM hydrogel as shown in Scheme 1.

PAM-Ag$^+$ Hydrogel was obtained by a two-step process. Firstly, the prepared PAM hydrogel was removed from the mold and dehydrated in an oven at 60 ℃ for 10 h. Secondly, the dried hydrogel was immersed into an $AgNO_3$ solution (1.0 mg/mL) for 12 h, forming the final PAM-Ag$^+$ Hydrogel.

Characterization

The morphologies of PAM and PAM-Ag$^+$ hydrogels were observed on the scanning electron microscope (Zeiss Merlin Compact). Before SEM observation, freezing and drying the hydrogels and then cutting out the section with a sharp knife to observe the internal structures of the hydrogels. Before testing, the sample surfaces were sprayed with gold. And the test voltage was 5.00 kV, and the magnification ratio was 3.24 KX. The tensile stress-strain curves were obtained using a tensile machine (Instron 5565a).

Mechanical Testing

All of the hydrogels were measured with a conventional test instrument at ambient temperature to test tensile strength. At first, a rectangular shape sample with 15 mm length, 5 mm width, 2 mm height was cut from a cylindrical hydrogel. Then, the prepared sample was placed between the jaws and at 180 mm/min crosshead speed until the hydrogel broke. Finally, the tensile stress (σ) of hydrogel was calculated according to the following description. $\sigma = F \cdot W \cdot H \cdot L / L_0$, where F, W, H, L_0, and L represent the force, width, height, and original length of the sample and the real-time length during the stretch process, respectively. And tensile strain (ε) is defined as the $\varepsilon = (L - L_0)/ L_0 \times 100\%$ [11,28].

Moisturizing Testing

Moisture retention of the hydrogels was evaluated by the amount of water loss in the hydrogel at a fixed time. PAM-Ag$^+$ Hydrogel with 5 mL water in a bottle had an original weight $M_{S,0}$, then it was replaced in an oven at 37 ℃ for 24 h with another weight $M_{S,1}$. Then, 5 mL water in the same bottle with an original weight $M_{C,0}$ was laid up in an oven at 37 ℃ for 24 h and had another weight $M_{C,1}$. All measurements were conducted three times to confirm the values. The Moisturizing rate was determined according to the equation: $MR\% = (M_{C,0}-M_{C,1}) - (M_{S,0}-M_{S,1})/(M_{C,0}-M_{C,1}) \times 100\%$.

Permeability Testing

The breathability of the hydrogels was measured by moisture permeability. Six sampling bottles adding 20 mL water with the same specification were taken and recorded M_0 respectively. The polyethylene (PE) film, PAM-Ag$^+$ Hydrogel, and medical gauze were with identical 1mm thickness sealed in the bottle mouth with S as the area. After laying in an oven at 37 ℃ for 24 h, the weight was recorded as M_1. All measurements were conducted three times to confirm the values. The breathability rate was calculated based on the formulae: $BR\ (g/m^2/24\ h^{-1}) = (M_0-M_1)/S$.

Watertightness Testing

The water-tightness of the hydrogels was preliminarily measured by the droplets of water passing through a hydrogel.

Swelling ratio

The swelling ratio of the hydrogels was estimated according to the amount of excess water absorbed. PAM-Ag^+ Hydrogels with an initial weight M_0 after being dried with filter paper, then immersed in excess water for 24 h with another weight M_1 after being dried with filter paper. All measurements were conducted three times to confirm the values. The permeability rate was determined according to the equation: $SR\% = (M_1-M_0)/M_0 \times 100\%$ [36].

Skin irritation testing

The skin irritation *in vivo* rat test was developed by 16 male white Guinea pigs weighing 250 ~ 300 g after raising for a week-appropriate environment and it included acute and secular tests, which all contained completed and impaired skin. As the completed skin irritation test, 8 Guinea pigs with the symmetrical part of both sides of back spine hair which was about 3×3 cm removed, and the PAM-Ag^+ Hydrogel (1.15 mM, 1×1×0.1 cm) was stuck to the Guinea pig removed from the left hair for 24 h, and removed by warm water. It compared with the completed right part of the Guinea pig after hydrogel was removed for 0, 24, 48 h and observed the local reaction of the skin with a result in the light of a standard of skin irritation. The impaired skin irritation was similar to the completed skin except the Guinea pig was handled with 75% alcohol disinfection and located by the tip of the syringe with the range of 1×1 cm. The differences between the acute and secular tests were the time which was 24 h and 14 d, respectively [37].

Skin sensitization testing

The Guinea pigs managed the skin sensitization *in vivo* rat test the same as the skin irritation. It contained sensitized and stimulated contact. As the sensitized contact, the positive group was as the followings, 0.2 mL 2-mercaptobenzothiazole (1%, 70% alcohol configuration) was applied evenly to exposed skin on the left side of the Guinea pig's back and removed with warm water after 6h. It repeated at the 7d and 14d. Another group was similar positive's sensitizer that 2-mercaptobenzothiazole was changed to the hydrogels as in the skin irritation handled. The stimulated contact was continued after the last sensitized test and alike operation on the Guinea pigs but on the right back. 24h, 48h, 72h after removing the medicine or hydrogels had a distinct evaluation with the same standard.

In vitro Col release

Release kinetics of the hydrogel was evaluated using Col as a model of acute gout for this work. The dried PAM hydrogel was placed into an aqueous solution containing 0.5 mg Col and $AgNO_3$ with a certain concentration. Then, the Col-loaded hydrogels were immersed in 100 mL PBS (Phosphate buffered saline, pH 7.4) solution. 1 mL of sample aliquot was taken out and replaced by an equal amount of fresh PBS solution. The Col contents were detected using an HPLC system consisting of an ultraviolet absorbance detector (Thermo Ultimate 3000) and a detection wavelength of 254 nm. The stationary phase was afforded with a Luna 5 μm C18(2) 100A, 250 x 4.6 mm, enclosed in a column oven equilibrated at 30℃. Solvent A was 100 % water, solvent B was 100 % methyl alcohol. The mobile phase (solvent A: solvent B = 40: 60, v/v) was eluted at 1 mL/min [38].

RESULTS AND DISCUSSIONS

Preparation of PAM and PAM-Ag^+ hydrogels

Traditional hydrogels adopted the way of chemical cross-linking. The cross-linking region of the whole hydrogel network was irregularly distributed due to the employment of organic cross-linkers, which led to the irregular spatial structure of the hydrogels, and the length of the segments between different crosslinking points was different during the polymerization. Finally, it was easier to break while load-bearing. Form a hydrogel with uniform internal spatial structure; thus, the energy generated when the gel deformation can be well-distributed consequently was important. The PAM hydrogel was synthesized by one-pot radical polymerization under UV irradiation as shown in Fig. S1.

BACA was used as a cross-linking agent which had a disulfide bond and possessed dynamic reversibility under ultraviolet light so that the hydrogel prepared had a homogeneous structure. The number of monomers, cross-linking agents and photo-initiators had a key influence on the mechanical strength of hydrogels, and the detailed analysis was shown in Table 1. Firstly, keeping the mass (M) of AM (1000 mg) and Irgacure 2959 (3 mg) constant, the effect of M_{BACA} on tensile stress and strain was given in Fig. 1a. It revealed that as the M_{BACA} increased from 0 to 1.5 mg, the tensile stress of PAM hydrogel improved gradually from 0.20 to 0.47 MPa, whereas the strain increased from 896 to 2907 %. However, when the M_{BACA} increased from 1.5 to 2.5 mg,

Table 1: The Proportion of each component in the PAM hydrogels.

Sample	AM (mg)	Irgacure 2959 (mg)	BACA (mg)	Stress (MPa)	Strain (%)
H1	1000	3.0	0.5	0.20	896
H2	1000	3.0	1.0	0.39	1318
H3	1000	3.0	1.5	0.47	2907
H4	1000	3.0	2.0	0.34	1062
H5	1000	3.0	2.5	0.34	1061
H6	800	3.0	1.5	0.14	1346
H7	1200	3.0	1.5	0.38	947
H8	1400	3.0	1.5	0.44	947
H9	1000	1.0	1.5	0.39	1617
H10	1000	5.0	1.5	0.23	1291

the tensile stress decreased from 0.47 to 0.34 MPa, the strain also decreased from 2907 to 1061 %. This was reasonable that the role of BACA was a chemical crosslinker, which added to provide proper mechanical strength and hold the shape of hydrogels, but too much BACA led to a higher crosslink density and inhibited the movement of the polymer chain, causing the brittleness of the structure. Secondly, keeping the M_{BACA} (1.5 mg), and Irgacure 2959 (3 mg) constant, the effect of M_{AM} on the mechanical strength of PAM hydrogel was also investigated and the results were shown in Fig. 1b. With the M_{AM} increased to 1000 mg, the tensile stress and strain of the PAM hydrogel achieved the maximum. Further expanding the M_{AM}, the strain decreased obviously because of the formation of too many PAM chains, causing the stiffness of hydrogel. Finally, as shown in Fig. 1c, it was clear that the tensile strength of PAM hydrogel was up first and then down when the $M_{Irgaure2959}$ increased. The amount of initiator determined the polymerization speed and length of the PAM chains. More initiators represented the easier activation of the vinyl groups of the AM, the faster formation of the PAM chain, and the shorter the length. Therefore, considering the mechanical strength of hydrogel, the contents of BACA, AM, and initiator were fixed at 1.5 mg, 1000 mg, and 3 mg for continued research.

To investigate the influence of disulfide bonds on the mechanical properties and internal structure of PAM hydrogels, different hydrogels were prepared with crosslinker BACA and MBA respectively as the amount of AM and initiator were the same. As shown in Fig. 2, the mechanical properties of PAM hydrogel using MBA were far less than those using BACA and correspond to the microstructures. After freeze-dry cycles, the morphology of hydrogels was observed by Scanning Electron Microscopy (SEM). It seemed obvious that the distribution of pores using MBA was much more heterogeneous than using BACA (Fig. 3) with excellent energy dissipation under external load.

To further enhance the mechanical properties and applications of PAM hydrogel, silver ion was investigated owing to its unique antibacterial properties and could form a coordination bond with sulfur. The way silver ion loaded was discussed via two kinds of PAM-Ag^+ hydrogel that contained one pot and two steps, respectively. The One-pot method was just taking $AgNO_3$ (1.15 mM) into the cylindrical mold with dissolved AM and BACA, and then added the desired initiator to polymerize for 30 min under UV irradiation. The two-step method was described in the experiment section. Tensile tests were carried out for the pure PAM hydrogel, the PAM hydrogel with Ag^+ loaded before polymerization (One-pot) and the PAM hydrogel with Ag^+ loaded after polymerization (Two-steps), respectively (Fig. 4a). The results showed that the tensile stress of pure PAM hydrogel was about 0.47 MPa at the elongation of 2907%. Adding Ag^+ before polymerization, the tensile strength and elongation of the prepared one-pot hydrogel decreased sharply in comparison with pure PAM hydrogel. This result indicated that the addition of Ag^+ before polymerization would change the stability of the internal structure. On the contrary,

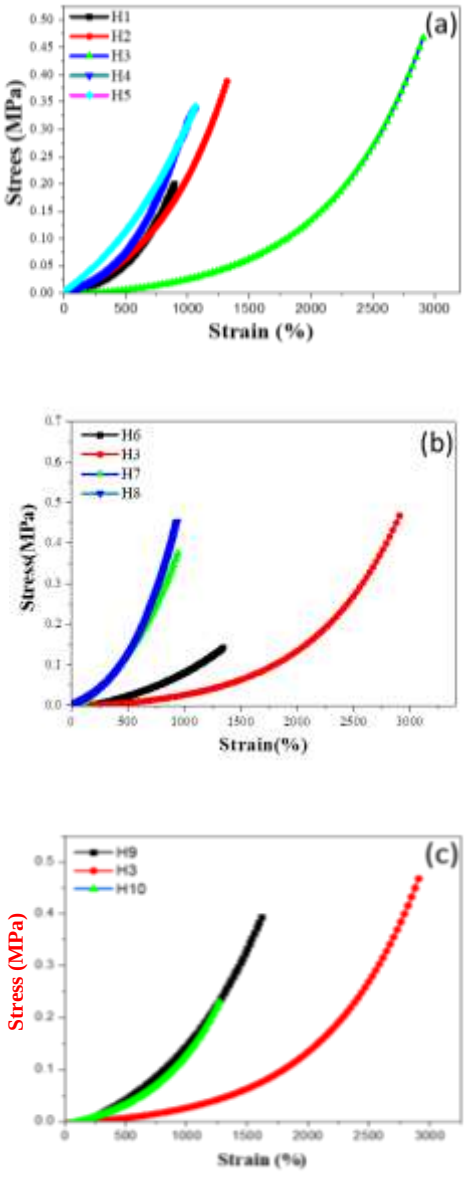

Fig. 1: Influence of different factors on the mechanical property of PAM hydrogel. (a) the concentration of BACA (b) the concentration of AM (c) the concentration of the initiator.

the tensile stress of the prepared two-steps hydrogel could achieve 2.55 MPa, which was 5.4 times higher than pure PAM hydrogel. More specially, the elongation has not been significantly reduced. Fig. 4b showed that both BACA and $AgNO_3$ solution was clear and transparent. When the two solutions were mixed, the resultant solution was found to be ivory, which is reasonable for the Ag-S coordination reaction that occurred (Fig. S2). These data intuitively demonstrate the significant role of introducing

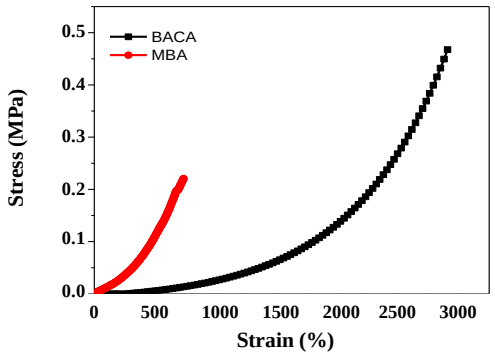

Fig. 2: Mechanical property of PAM hydrogel with different types of crosslinking agents.

silver ions after polymerization in enhancing the mechanical strength of the hydrogel that would not affect the homogeneous network originally formed in the hydrogel and made for metal coordination bonds formed, which completely accumulated the mechanical strength of PAM hydrogel.

Adhesion properties of PAM-Ag^+ hydrogel

To clearly illustrate the adhesive performance of high-strength hydrogel in medical dressing, the macroscopic stretching and adhesion processes were displayed. As shown in Figs. 5a and 5b, the PAM-Ag^+ hydrogel with its original 5 cm length and 2.5 cm wide was approximately stretched to 28 cm length and 7 cm wide and exhibited impressive areas expansion (~1570%) without obvious breakage. The excellent tensile performance mainly depended on the uniform structure of the hydrogel and it could be stretched to any other shape as required. The PAM-Ag^+ hydrogel possessed outstanding ductility and flexibility that could be fixed to the human forearm and any part of the skin such as the finger and elbow joint (Figs. 5c-5g), the hydrogel had a favorable capacity to withstand huge deformation mainly due to the Ag-S coordination dynamically.

Properties of PAM-Ag^+ hydrogel for medical dressing

The properties of PAM-Ag^+ hydrogel were significantly important for medical dressing, especially the moisture retention, permeability, water tightness, and swelling ratio. Water loss and moisture of different silver ion concentration hydrogels in 24 h were compared in Fig. 6, and the corresponding results were summarized in Table 2. After being replaced in an oven at 37 ℃ for 24 h,

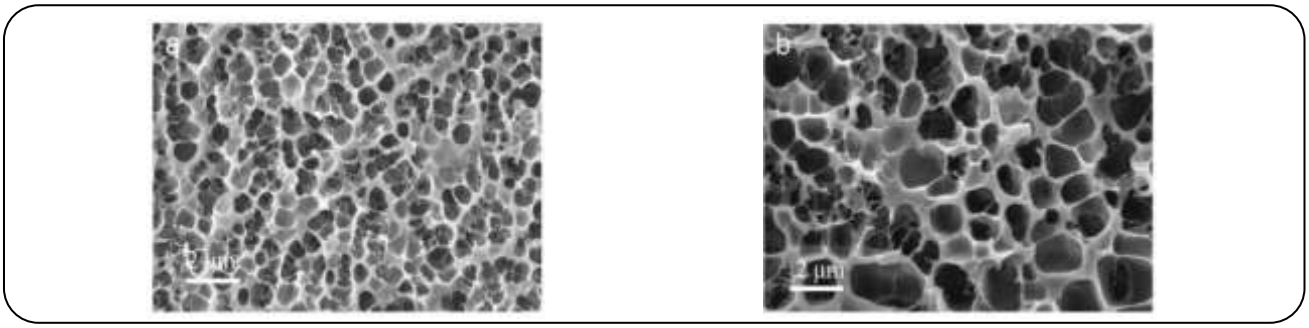

Fig. 3: SEM images of PAM hydrogel. (a) crosslinked by BACA; (b) crosslinked by MBA.

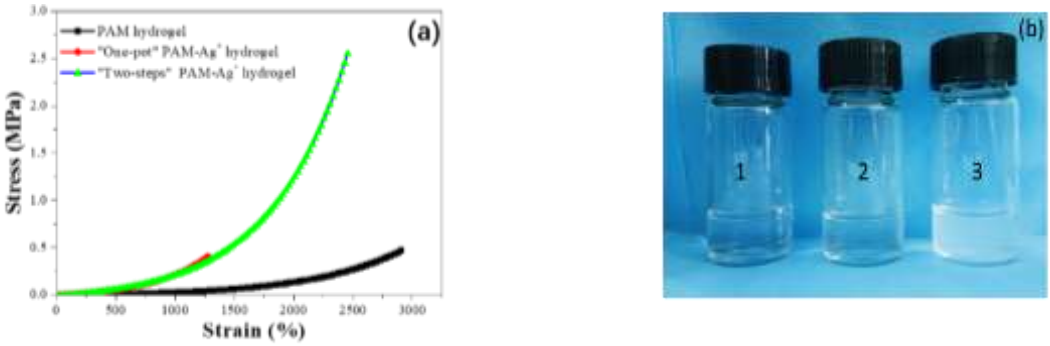

Fig.4. Effects of silver ion on the mechanical strength of hydrogels. (a) the mechanical property of PAM and PAM-Ag^+ hydrogels with different methods. (b)1 represented the BACA solution, 2 represented the $AgNO_3$ solution, 3 represented the $AgNO_3$-BACA solution.

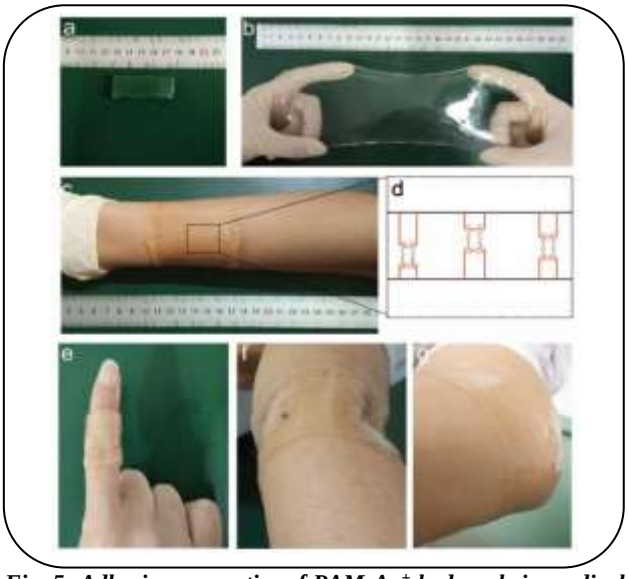

Fig. 5: Adhesion properties of PAM-Ag^+ hydrogels in medical dressing.

the hydrogels still retained a certain amount of water. PAM-Ag^+ hydrogels reduced moisture volatilization by nearly half in the same condition and different silver content had almost little effect on the water retention performance of hydrogels. The Denser pore structure made PAM-Ag^+ hydrogel a good moisturizer.

Medical textiles need to be effective in preventing water penetration outside. The water repellency of the hydrogels was preliminarily measured by the droplets of water passing through the gauze (Fig. S3a) and hydrogel (Fig. S3b). It was obvious that water droplets could easily fall into the vessel through the gauze layer while the vessel with hydrogel on the surface could not. It was undoubted that the water resistance of hydrogel was much better than medical gauze and prevented water from entering the wound.

To clearly illustrate the breathability of the hydrogels, PE film, and medical gauze with the same thickness were chosen to compare. Water vapor permeability is an index to measure the gas permeability of hydrogels. As shown in Fig. 7a, PE film was approximatively watertight but the hydrogels with different silver ion concentrations were almost the same as medical gauze and had favorable gas permeability. Detailed results were summarized in Table 3. Water vapor permeability in 24 h of PE film was about 9.55 g/m^2, but the hydrogels researched were up above 400 g/m^2 which was the same

Table 2: The Moisture of PAM-Ag⁺ hydrogels (n=3).

	Pure water	Silver ion concentration of PAM-Ag⁺ hydrogel（mM）			
		0	0.115	0.23	1.15
Water loss in 24 h（g）	4.26 ± 0.21	2.17 ± 0.39	2.16 ± 0.21	2.05 ± 0.33	2.24 ± 0.43
Moisturizing efficiency（%）	-	49.06 ± 9.06	49.30 ± 4.88	51.80 ± 7.63	47.50 ± 10.10

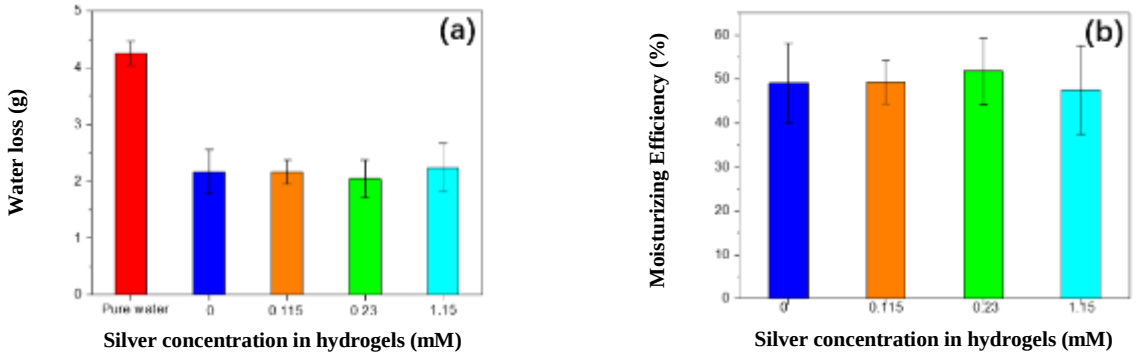

Fig. 6: The moisture of PAM-Ag⁺ hydrogel (a) Water loss in 24 h (b) Moisturizing efficiency of PAM-Ag⁺ hydrogel with different silver ion concentrations. (n=3, Error bars show the standard deviations).

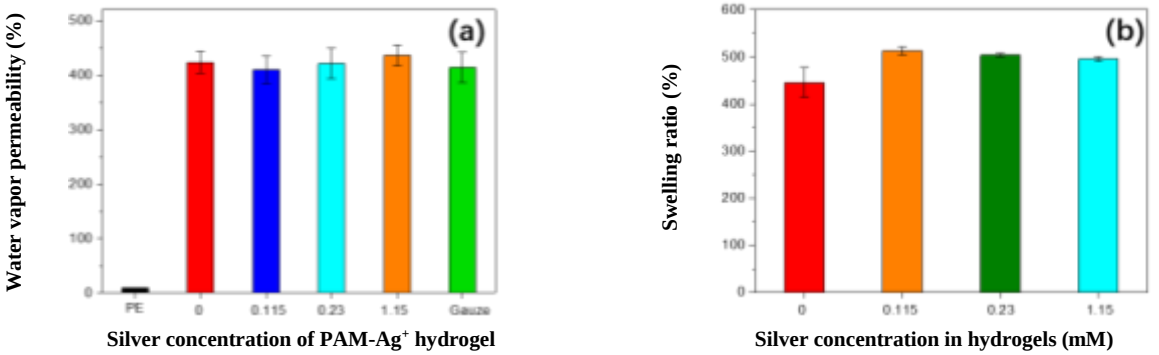

Fig. 7: The permeability (a) and swelling properties (b) of PAM-Ag⁺ hydrogels. (n=3, Error bars show the standard deviations).

as the medical gauze. Compared with the PE film, PAM-Ag⁺ hydrogels were much better and the silver concentration had almost no contributions according to the statistical analysis. Since their great hydrophilic property (Fig. S4), the Swelling Ratio (SR) was one of the most important factors to evaluate hydrogels. As shown in Table S1, it could be found that the swelling capability of PAM-Ag⁺ hydrogel far exceeded pure PAM hydrogel which was attributed to the uniform structure. The SR of adhesive PAM-Ag⁺ hydrogel could reach nearly 500% after being immersed in water for 24 h (Fig. 7b). Statistical analysis results showed that the concentrations of silver ions had little effect on the swelling ratio of hydrogels and it's because silver ions had weak influences on pore structure.

Biocompatibility evaluation of PAM-Ag⁺ hydrogels

Biocompatibility was one of the most important prerequisites for the safe use of medical dressings. Skin irritation and sensitization tests were parts of the initial evaluation laid down in ISO standards on the biological evaluation of medical dressings and performed according to ISO 10993-10 to evaluate the *in vitro* safety of the hydrogel for further clinical investigation. Guinea pigs are anatomically similar to humans with thicker, denser cuticles and almost identical cell renewal rates.

Table 3: The gas permeability of PAM-Ag^+ hydrogels (n=3).

	PE film	Silver ion concentration of PAM-Ag^+ hydrogel（mM）				Medical gauze
		0	0.115	0.23	1.15	
Water vapor permeability (g/m^2/24 h)	9.55 ± 0	423.57 ± 19.89	409.77 ± 24.74	421.44 ± 28.32	436.31 ± 19.11	414.01 ± 27.76

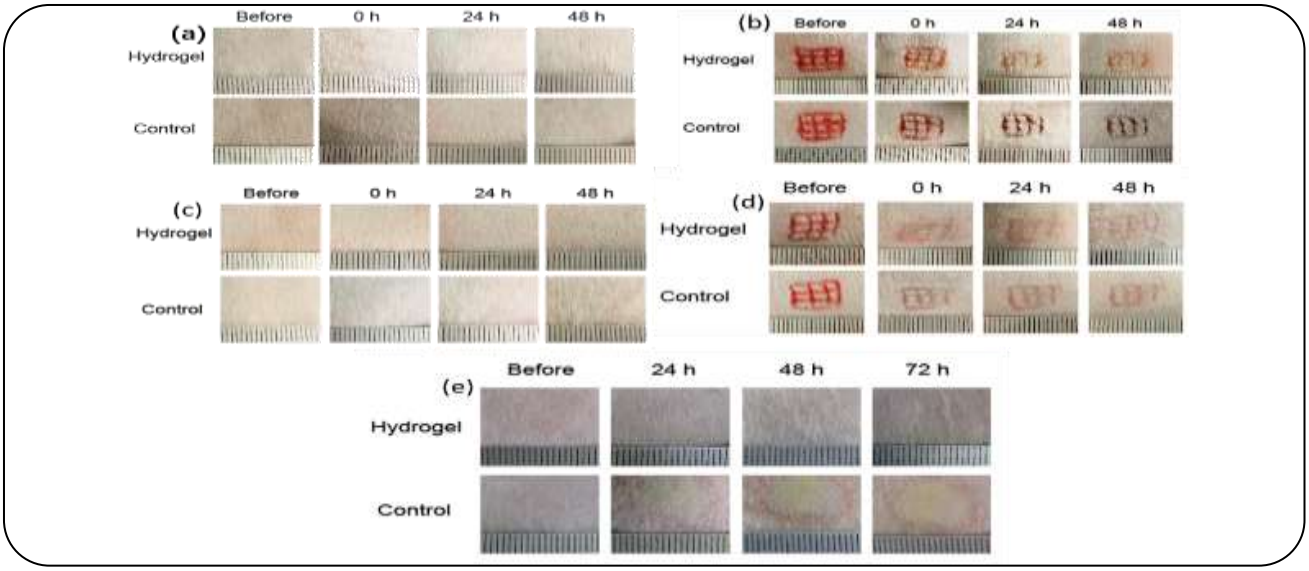

Fig.8. The images of Skin irritation and sensitization tests of Guinea pig (a) short-term skin irritation on complete skin (b) short-term skin irritation on damaged skin (c) long-term skin irritation on complete skin (d) long-term skin irritation on damaged skin (e) skin sensitization.

The Guinea pigs implanted in two groups were healthy and no signs of inflammation were observed. As shown in Figs. 8a and 8b, PAM-Ag^+ hydrogel with 1.15 mM Ag^+ was used in comparison to the blank control group, and there were no significant disparities from the images which meant no irritation with normal and damaged skin using hydrogels acutely. The results of short-term skin irritation on complete and damaged skin were summarized in Table S2 according to the standards (Table S3 and S4). Surprisingly, after using the hydrogels for 14 days, there was no irritation yet (Figs. 8c and 8d) and the evaluation findings were listed in Table S5. Skin sensitization was studied by comparing with the positive group using 2-mercaptobenzothiazole as the sensitizing agent. Whether sensitized or stimulated with the PAM-Ag^+ hydrogel, the sensitization rate was zero but the positive group was 100 % (Fig. 8e). Contrasted with the classification of sensitization rate, the hydrogel couldn't induce skin allergy with I level but 2-mercaptobenzothiazole was easy to induce skin allergy so the level was V according to Table S6 as the elaborate evaluation findings were listed in Table S7 based on the standards (Table S8).

In vitro Col release

Colchicine was chosen here as a model drug for the drug release study. Colchicine has an excellent effect on acute gout attacks. However, the potential side effects related to its oral administration and the speedy elimination from the body limited its utilization. The *in vitro* release rate of Col was carried out as the different content of silver ion. As shown in Fig. 9, free Col showed a rapid release rate during the first 10 min, approximately 60 % of the cumulative release. All the hydrogel systems exhibited burst in the first 3 h and about 40 % of loaded Col was released, thereafter the Col release quantity significantly increased with prolonged-release time. As the silver ion concentration was 0.115 mM, more than 95% of loaded Col was released within 48 h. The results may be explained by the drug encapsulation in the form of the Col-Ag^+ complex, as the complexes entrapped in the network,

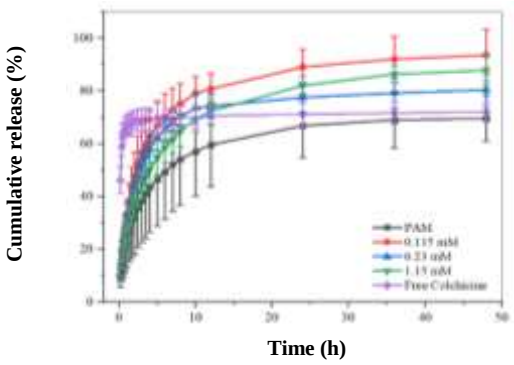

Fig. 9: In vitro drug release of hydrogels with the influence of Ag^+ concentration (n=3, Error bars show the standard deviations).

the Ag^+ would coordinate with the sulfur atoms of the BACA while dynamic metal coordination Ag^+-S formed, revealing a dissociative-free drug. When the content of Ag^+ increased to 0.23 mM, the free drug content decreased while the release quantity was approximately 80%. Such results suggest that the hydrogel can be tuned to provide appropriate sustained drug release systems.

CONCLUSIONS

In summary, a well-defined network hydrogel with excellent mechanical, and adhesive properties is successfully prepared for medical dressing and drug delivery systems. By introducing silver ions into the PAM hydrogel network, a highly mechanical and stretchable PAM-Ag^+ hydrogel was prepared. The PAM-Ag^+ hydrogel shows high strength of 2.55 MPa along with good flexibility of about ~2600% based on PAM hydrogel accompanied with 0.46 MPa strength. Meanwhile, the PAM-Ag^+ hydrogel has demonstrated its great promise for surgical wound dressings due to its strongest mechanical, great moisture, permeability, swelling properties, and no short-term, or long-term skin irritation and sensitization. Additionally, the PAM-Ag^+ hydrogel exhibited excellent sustained-release properties and up to 90 % drug release as loaded with Col.

Funding Statement

This research was funded by the National Natural Science Foundation of China (Grants 21802001), the Anhui Provincial Natural Science Foundation (Grants 1808085QB52), the Anhui Provincial Education Department Natural Science Key Foundation (Grants KJ2021A0596), and the Foundation of Anhui Province Key Laboratory of Research & Development of Chinese Medicine (Grants AKLPDCM202309).

Received : Jul. 13, 2021 ; Accepted : Oct. 18, 2021

REFERENCES

[1] Giampiero G., Gianpaolo T., Jan D.B., The Skin as an Immunologic Organ, *Handbook of Systemic Autoimmune Diseases*, **5**: 3-9 (2006).

[2] Qu J., Zhao Y., Liang Y., Xu P.X., Ma B.G., Degradable Conductive Injectable Hydrogels as Novel Antibacterial, Anti-Oxidant Wound Dressings for Wound Healing, *Chemical Engineering Journal*, **362**: 548-560 (2019).

[3] Sandra A., Nordin A., Hwei N.M., Chin Kok-Yong, Abd Aziz I.F., Mh B., Natural 3D-Printed Bioinks for Skin Regeneration and Wound Healing: A Systematic Review, *Polymers*, **12(8)**: 1782 (2020).

[4] Shen Z., Cai N., Xue Y.N., Chan V., Yu B., Wang J.Z., Song H., Deng H., Yu F.Q., Engineering Sustainable Antimicrobial Release in Silica-Cellulose Membrane with $CaCO_3$-Aided Processing for Wound Dressing Application, *Polymers*, **11(5)**: 808 (2019).

[5] Chen R.K., Zhu Z.Y., Ji S.F., Geng Z.J., Hou Q., Sun X.Y., Fu X.B., Sweat Gland Regeneration: Current Strategies and Future Opportunities, *Biomaterials*, **255**: 120201 (2020).

[6] Boateng J.S., Matthews K.H., Stevens H.N.E., Eccleston G.M., Wound Healing Dressings and Drug Delivery Systems: A Review, *Journal of Pharmaceutical Sciences*, **97(8)**: 2892-2923 (2008).

[7] Khan M.A., Maqsoodur R.W., Ahmed H., Khan A., Ahmad M., Khan J., Development of Diclofenac Sodium Matrix Tablets Using Sunflower Stem Residue, *American Journal of Pharmacy and Health Research*, **2(7)**: 278-289 (2014).

[8] Roel C. Op't Veld, Walboomers X.F., Jansen J.A., Wagener F.A.D.T.G., Design Considerations for Hydrogel Wound Dressings; Strategic and Molecular Advances, *Tissue Engineering Part B*, **26(3)**: 230-248 (2020).

[9] Peng Y.L., Wang Z.F., Zhou Y., Wang F.Y., Zhang S.N., He D.G., Deng L., Ferrocene-Functionalized Hybrid Hydrogel Dressing with High-Adhesion for Combating Biofilm, *Materials Science & Engineering C*, **125**: 112111 (2021).

[10] Mojtaba F., Abbas S., Wound Healing: Form Passive to Smart Dressings, *Advanced Healthcare Materials*, **10(16)**: 2100477 (2021).

[11] Chen T., Chen Y.J., Rehman H.U., Chen Z., Yang Z., Wang M., Li H., Liu H.Z., Ultratough, Self-Healing, and Tissue-Adhesive Hydrogel for Wound Dressing, *ACS Applied Materials & Interfaces*, **10(39)**: 33523-33531 (2018).

[12] Li J.Y., Mooney D.J., Designing Hydrogels for Controlled Drug Delivery, *Nature Reviews Materials*, **1(12)**: 16071 (2016).

[13] Zhao X.D., Pei D.D., Yang Y.X., Xu K., Yu J., Zhang Y.C., Zhang Q., He G., Zhang Y.F., Li A., Cheng Y.L., Chen X.S., Green Tea Derivative Drove Smart Hydrogels with Desired Functions for Chronic Diabetic Wound Treatment, *Advanced Functional Materials*, **31(18)**: 2009442 (2021).

[14] Chen C., Yang X., Li S.J., Zhang C., Ma Y.N., Ma Y.X., Gao P., Gao S.Z., Huang X.J., Tannic Acid-Thioctic Acid Hydrogel: A Novel Injectable Supramolecular Adhesive Gel for Wound Healing, *Green Chemistry*, **23(4)**: 1794-1804 (2021).

[15] Chen H., Cheng R.Y., Zhao X., Zhang Y.H., Tam A., Yan Y.F., Shen H.K., Zhang Y.S., Qi J., Feng Y.G., Liu L., Pan G.Q., Cui W.G., Deng L.F., An Injectable Self-Healing Coordinative Hydrogel with Antibacterial and Angiogenic Properties for Diabetic Skin Wound Repair, *NPG Asia Materials*, **11(1)**: 3 (2019).

[16] Kazutoshi H., Toru T., Nanocomposite Hydrogels: A Unique Organic-Inorganic Network Structure with Extraordinary Mechanical, Optical, and Swelling De-swelling properties, *Advanced Materials*, **14(16)**: 1120-1124 (2002).

[17] Jiao C., Zhang J.N., Liu T.Q., Peng X., Wang H.L., Mechanically Strong, Tough and Shape Deformable Poly(Acrylamide-Co-Vinyl Imidazole) Hydrogels Based on Cu Complexation, *ACS Applied Materials & Interfaces*, **12(39)**: 44205-44214 (2020).

[18] Yang C.H., Wang M.X., Haider H., Yang J.H., Sun J.Y., Chen Y.M., Zhou J.X., Suo Z.G., Strengthening Alginate/Polyacrylamide Hydrogels Using Various Multivalent Cations, *ACS Applied Materials & Interfaces*, **5(21)**: 10418-10422 (2013).

[19] Stephan H., Agmal S., Michael K., Silke H., Antje T., Katrin F., Christian G., Christian K., Rudolf H., Norbert K., Silver Nanoparticles: Evaluation of DNA Damage, Toxicity and Functional Impairment in Human Mesenchymal Stem Cells, *Toxicology Letters*, **201(1)**: 27-33 (2011).

[20] Tang Q.Q., Chen C.W., Jiang Y.G., Huang J.J., Liu Y., Nthumba P.M., Gu G.S., Wu X.W., Zhao Y., Ren J.N., Engineering an Adhesive Based on Photosensitive Polymer Hydrogels and Silver Nanoparticles for Wound Healing, *Journal of Material Chemistry B*, **8(26)**: 5756-5764 (2020).

[21] Han L., Lu X., Liu K.Z., Wang K.F., Fang L.M., Weng L.T., Zhang H.P., Tang Y.H., Ren F.Z., Zhao C.C., Sun G.X., Liang R., Li Z.J., Mussel-Inspired Adhesive and Tough Hydrogel Based on Nanoclay Confined Dopamine Polymerization, *ACS Nano*, **11(3)**:2561−2574 (2017).

[22] Chen C.Y., Yin H., Chen X., Chen T.H., Liu H.M., Rao S.S., Tan Y.J., Qian Y.X., Liu Y.W., Hu X.K., Luo M.J., Wang Z.X., Liu Z.Z., Cao J., He Z.H., Wu B., Yue T., Wang Y.Y., Xia K., Luo Z.W., Wang Y., Situ W.Y., Liu W.E., Tang S.Y., Xie H., Angstrom-Scale Silver Particle-Embedded Carbomer Gel Promotes Wound Healing by Inhibiting Bacterial Colonization and Inflammation, *Science Advances*, **6(43)**: eaba0942 (2020).

[23] Alexandra E.S., Cristina C., Alexandru M.G., Nanomaterials for Wound Dressings: An Up-to-Date Overview, *Molecules*, **25(11)**:2699-2724 (2020).

[24] Boateng J.S., Matthews K.H., Stevens H.N.E., Eccleston G.M., Wound Healing Dressings and Drug Delivery Systems: A Review, *Journal of Pharmaceutical Sciences*, **97(8)**: 2892-2923 (2008).

[25] Liu W.J., Sun J., Sun Y., Xiang Y., Yan Y.F., Han Z.H., Bi W., Yang F., Zhou Q.R., Wang L., Yu Y.C., Multifunctional Injectable Protein-Based Hydrogel for Bone Regeneration, *Chemical Engineering Journal*, **394**:124875 (2020).

[26] Chen Z.M., Cai Z.W., Zhu C.J., Song X.M., Qin Y.H., Zhu M.H., Zhang T., Cui W.G., Tang H.H., Zheng H.L., Antibacterial Hydrogels: Injectable and Self-Healing Hydrogel with Anti-Bacterial and Anti-Inflammatory Properties for Acute Bacterial Rhinosinusitis with Micro Invasive Treatment, *Advanced Healthcare Materials*, **9(20)**:2070073 (2020).

[27] Xu F., Padhy H., Al-Dossary M., Zhang G.S., Behzad A.R., Stingl U., Rothenberger A., Synthesis and Properties of the Metallo-Supramolecular Polymer Hydrogel Poly[Methyl Vinyl Ether-Alt-Mono-Sodium Maleate]Center dot $AgNO_3$: Ag^+/Cu^{2+} Ion Exchange and Effective Antibacterial Activity, *Journal of Materials Chemistry B*, **2(37)**:6406-6411 (2014).

[28] Qin H.L., Zhang T., Li H.N., Cong H.P., Antonietti M., Yu S.H., Dynamic Au-Thiolate Interaction Induced Rapid Self-Healing Nanocomposite Hydrogels with Remarkable Mechanical Behaviors, *Chemistry*, **3(4)**: 691-705 (2017).

[29] Song P., Qin H.L., Gao H.L., Cong H.P., Yu S.H., Self-Healing and Super Stretchable Conductors from Hierarchical Nanowire Assemblies, *Nature Communications*, **9**: 2786 (2018).

[30] Qin H.L., Zhang T., Li N., Cong H.P., Yu S.H., Anisotropic and Self-Healing Hydrogels with Multi-Responsive Actuating Capability, *Nature Communications*, **10**: 2202 (2019).

[31] Hussain I., Sayed S.M., Liu S.L., Yao F., Oderinde O., Fu G.D., Hydroxyethyl Cellulose-Based Self-Healing Hydrogels with Enhanced Mechanical Properties *via* Metal-Ligand Bond Interactions, *European Polymer Journal*, 100:219-227 (2018).

[32] Chen X.Q., Song Z.H., Li S.P., Thang N.T., Gao X., Gong X.C., Guo M.H., Facile One-Pot Synthesis of Self-Assembled Nitrogen-Doped Carbon Dots/Cellulose Nanofibril Hydrogel with Enhanced Fluorescence and Mechanical Properties, *Green Chemistry*, **22**: 3296-3308 (2020).

[33] Xu J.J., Wang G.Y., Wu Y.F., Ren X.Y., Gao G.H., Ultrastretchable Wearable Strain and Pressure Sensors Based on Adhesive, Tough, and Self-healing Hydrogels for Human Motion Monitoring, *ACS Applied Materials & Interfaces*, **11(28)**: 25613-25623 (2019).

[34] Dead H., Benyoucef A., Morallón E., Montilla F., Reactive Insertion of PEDOT-PSS in SWCNT@Silica Composites and its Electrochemical Performance, *Materials*, **13(5)**: 1200-1210 (2020).

[35] Chen H., Peng C., Wang L., Li X.X., Yang M., Liu H.H., Qin H.L., Chen W.D., Mechanically Tough, Healable Hydrogels Synergistically Reinforced by UV-Responsive Crosslinker and Metal Coordination Interaction for Wound Healing Application, *Chemical Engineering Journal*, **403**: 126341 (2021).

[36] Alamar A., Park S.H., Ibrahim I., Arun D., Holtz T., Dumee L.F., Lim H.N., Szekely G., Architecting Neonicotinoid-Scavenging Nanocomposite Hydrogels for Environmental Remediation, *Applied materials today*, **21**: 100878 (2020).

[37] Hong Y., Zhou F.F., Hua Y.J., Zhang X.Z., Ni C.Y., Pan D.H., Zhang Y.Q., Jiang D.M., Yang L., Lin Q.N., Zou Y.W., Yu D.S., Arnot D.E., Zou X.H., Zhu L.Y., Zhang S.F., Ouyang H.W., A strongly Adhesive Hemostatic Hydrogel for the Repair of Arterial and Heart Bleeds, *Nature Communications*, **10(1)**: 2060 (2019).

[38] Cankaya N., Bulduk I., Colak A.M., Extraction, Development and Validation of HPLC-UV Method for Rapid and Sensitive Determination of Colchicine from Colchicum Autumnale L. Bulbs, *Saudi Journal of Biological Sciences*, **26(2)**: 345-351 (2019).